ADVANCED ENGINEERING MATERIALS

DOI: 10.1002/adem.200800104

Thermoplastic Forming Properties and Microreplication Ability of a Magnesium-Based Bulk Metallic Glass**

By *Jason Shian-Ching Jang,* Chin-Tsung Tseng, Liang-Jan Chang, Jacob Chih-Ching Huang, Ya-Ching Yeh* and *Jin-Long Jou*

The thermoplastic forming properties in the supercooled liquid region of $Mg_{58}Cu_{31}Nd_5Y_6$ bulk metallic glass (BMG) rods were systematically characterized by thermal mechanical analysis (TMA) and compressive tests at different temperature with various strain rates. The process window of thermoplastic forming for the $Mg_{58}Cu_{31}Nd_5Y_6$ BMG was developed according to the results of TMA and the compressive tests. All evidence reveals that the $Mg_{58}Cu5_{31}Nd_5Y_6$ BMG possesses excellent superplastic formability with the *m* value being nearly 1.0 in the supercooled liquid region of 430–503 K under a strain rate around 2.5×10^{-3}–1.0×10^{-2} s^{-1}. In parallel, a relatively low flow stress (less than 10 MPa) within the supercooled liquid region can be obtained with a strain rate of 2.5×10^{-3} s^{-1}. Additionally, the replication of a hologram pattern with 100 nm depth also demonstrates extremely good microforming ability of this Mg-based BMG in the supercooled liquid region.

Magnesium alloys have attracted great attention in the category of engineering materials in recent years because of their high specific strength/density ratio and high damping capacity.[1–3] However, the inherent of low stiffness and poor workability of conventional magnesium alloys has resulted in its limited application up to now. Therefore, the development of high specific strength Mg-based bulk metallic glasses (BMGs) for application as structural materials is an important research topic. Recently, Inoue et al.[4,5] first found that Mg-Cu-Y ternary alloys exhibited high glass-forming ability (GFA) and can be produced as a BMG rod with a diameter of 7 mm by using copper mold-casting and high-pressure die-casting methods. Moreover, further improvement of the GFA has been reported by partially replacing Cu with a TM (TM: transition metal such as Ag, Pd, or Zn) in the Mg-Cu-Y alloy system, for example, $Mg_{65}Cu_{15}Ag_{10}Y_{10}$,[6,7] $Mg_{65}Cu_{20}Zn_5Y_{10}$,[8] and $Mg_{65}Cu_{15}Ag_5Pd_5Y_{10}$.[9,10] Additionally, the significant improvement of their GFA has been reported by adding a rare-earth element (Gd, Nd, Tb, Pr, or Dy) and lowering the amount of Mg in the Mg-based amorphous materials, such as Mg-Cu-Y-Gd,[11,12] Mg-Cu-Ni-Gd,[13] Mg-Cu-RE (RE = rare-earth element),[14] $Mg_{54}Cu_{28.5}Ag_{8.5}Gd_{11}$,[15] Mg-Cu-Gd-Nd,[16,17] and Mg-Cu-Y-Nd [18] alloy systems. All of these Mg-based BMGs exhibit high compressive fracture strength over 800 MPa,[19–21] which is twice the highest strength of conventional Mg-based crystalline alloys. In addition, these Mg-based BMGs usually present significant plasticity in supercooled liquid region (SCL) with behavior similar to a Newtonian viscosity of conventional glass materials, that is, the strain rate sensitivity exponent (*m*) is near 1. Hence, because of the superplastic deformation ability in the SCL region, Mg-based BMGs are capable of being manufactured into near-net-shape components, particularly for complex-shaped microcomponents for micro-electromechanical systems (MEMS).[22–25] The purpose of the present study is to establish the process window for microforming the $Mg_{58}Cu_{31}Nd_5$ Y_6 BMG (which possesses a high GFA) by means of a thermal mechanical analyzer (TMA) and a hot compression test at various temperature and strain rates. In parallel, a replication of microscaled hologram pattern by hot-pressing this Mg-based BMG in the SCL region is demonstrated herein.

Experimental

The composition of $Mg_{58}Cu_{31}Y_6Nd_5$ by atomic percentage was selected as the raw alloy for preparing the BMG specimen. High-purity Cu, Y, and Nd (> 99.9 %) were pre-alloyed into a Cu-Y-Gd master alloy by arc melting in a Ti-gettered argon atmosphere. Then, the Cu-Y-Gd alloy was melted together with high-purity Mg pieces to obtain an alloy ingot with the target composition by induction melting under an

[*] *Dr. J. S.-C. Jang, Mr. C.-T. Tseng, Dr. L.-J. Chang*
I-Shou University
Department of Materials Sci. & Eng.
Kaohsiung, Taiwan 84008, R.o.C.
E-mail: scjang@isu.edu.tw
Dr. J. C.-C. Huang
Institute of Materials Sci. & Eng.
Center for Nanoscience and Nanotechnology
National Sun Yat-Sen University
Kaohsiung, Taiwan 804, R.o.C.
Ms. Y.-C. Yeh, Dr. J.-L. Jou
Metal Industries Research & Development Centre
Kaohsiung, Taiwan 81160, R.o.C.

[**] *We gratefully acknowledge sponsorship from the National Science Council of RoC under the project NSC95-2221-E-214-015, and NSC96-2218-E-110-001. We are also very grateful for the assistance in TEM by the Micro and Nano Laboratory, Department of Materials Science and Engineering, I-Shou University.*

WILEY InterScience DISCOVER SOMETHING GREAT
© 2008 WILEY-VCH Verlag GmbH & Co. KGaA, Weinheim

argon atmosphere. The alloy ingots were remelted by induction melting in a quartz tube and injected into a water-cooled Cu mold by argon pressure to obtain BMG rods 4 mm in diameter and 50 mm long.

The thermal properties of the BMG sample was characterized by DSC (differential scanning calorimeter, TA Instruments DSC 2920) and TMA (thermal mechanical analyzer, Perkin–Elmer Diamond TMA) under flowing purified argon with a heating rate of 20 K/min. Several temperatures between glass transition temperature (T_g) and crystallization temperature (T_x) (namely 443, 448, 453, and 458 K) were selected for high-temperature compression tests by a MTS-810 mechanical test system with strain rates of 1×10^{-3}–1×10^{-2} s^{-1} to study the deformation behavior within the SCL region. The compression samples with the height-to-diameter ratio of 2:1 ($h = 8$ mm and $d = 4$ mm) were cut to be parallel from the as-cast $Mg_{58}Cu_{31}Y_6Nd_5$ BMG rod and carefully polished to ensure the flatness. Micro-forming ability was tested by hot pressing the BMG rod on a mold with laser-engraved hologram (with 10 mm depth of groove) at the SCL temperature region. Finally, the hot-compressed samples were examined by X-ray diffraction (Scintag X-400 X-ray diffractometer) with monochromatic Cu-K radiation. The micro-formed sample was examined by scanning electron microscopy (SEM).

Results and Discussion

The DSC and TMA curves of the $Mg_{58}Cu_{31}Y_6Nd_5$ BMG with a heating rate of 0.33 Ks^{-1} and l00 mN stress (7.96 kPa s) are illustrated as Figure 1. When the temperature is lower than T_g, the linear coefficient of thermal expansion (CTE) for an amorphous solid (α_{glass}) is 1.78×10^{-6} K^{-1}. As the temperature exceeds T_x, the CTE for crystalline solid ($\alpha_{crystal}$) changes to 5.85×10^{-5} K^{-1}, which is similar to that of common Mg alloys. In addition, the relative displacement as a function of temperature obtained from the TMA for the $Mg_{58}Cu_{31}Y_6Nd_5$ BMG rod with different compressive stress (7.96, 15.92, 23.88, 39.8, and 79.6 kPa) at the heating rate of 0.67 Ks^{-1} is shown in Figure 2. The relative displacement with increasing temperature is enhanced appreciably as the magnitude of loading increases, especially approaching the value of T_{onset}. The results in Figure 2 were converted into a plot of viscosity versus temperature by the equation

$$\eta = \frac{\sigma_{flow}}{\dot{\varepsilon}} \tag{1a}$$

in which σ_{flow} is flow stress and $\dot{\varepsilon}$ is strain rate, as shown in Figure 3. There is a clear viscosity transition at T_g; the glassy solid is rigid at temperatures below T_g and becomes viscous in the supercooled liquid region. A relatively low viscosity between 10^6 and 10^7 Pa·s occurs at the temperature interval of supercooled liquid region. As the temperature approaches T_x (about 490 K), the viscosity of the BMG sample increases rapidly back to 10^{10} Pa·s owing to the crystallization and becomes rigid matter again.

On the basis of the results from TMA, the viscous flow behavior of $Mg_{58}Cu_{31}Y_6Nd_5$ BMG rods were investigated by compression tests at various temperatures near T_{onset} with different strain rates (2.5×10^{-3}–1×10^{-2} s^{-1}) in the SCL region. The true stress–strain curves of the BMG samples deformed at 438, 448, 453, and 458 K with different strain rates between 2.5×10^{-3} and 1×10^{-2} s^{-1} are summarized in Figure 4. Most of

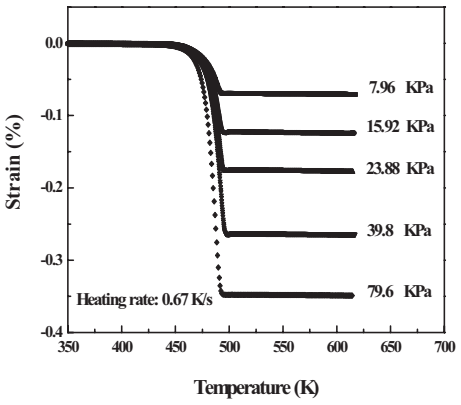

Fig. 2. TMA curves for the $Mg_{58}Cu_{31}Y_6Nd$ BMG rods with different compressive stress (namely, 7.96, 15.92, 23.88, 39.8, and 79.6 kPa) at a heating rate of 0.67 K s^{-1}.

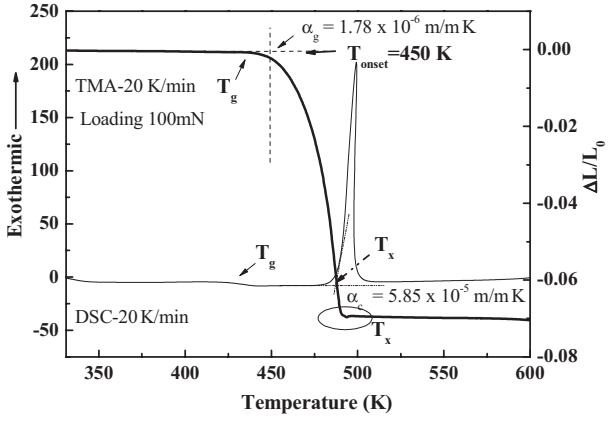

Fig. 1. DSC and TMA curves for the $Mg_{58}Cu_{31}Y_6Nd_5$ BMG rod.

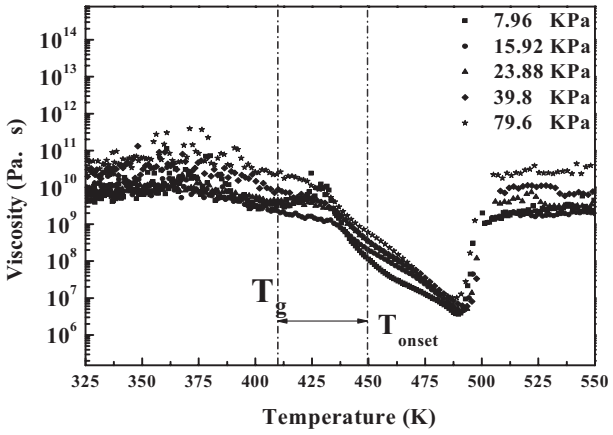

Fig. 3. Viscosity with increasing temperature at different compression stress for the $Mg_{58}Cu_{31}Y_6$ Nd_5 BMG rod.

 © 2008 WILEY-VCH Verlag GmbH & Co. KGaA, Weinheim

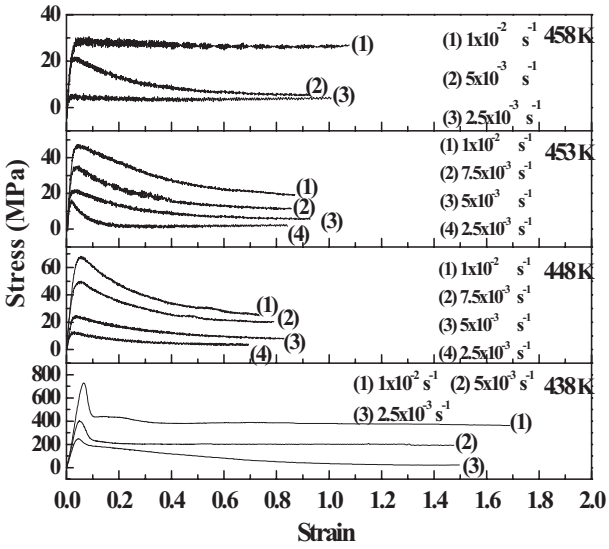

Fig. 4. True stress–strain curve of compression test for $Mg_{58}Cu_{31}Y_6$ Nd_5 amorphous alloy at different temperatures.

stress–strain curves show a sharp peak of stress at the beginning of compression and the stress significantly reduces to a stable and relatively low value with increasing plastic strain. In addition, the flow stress also decreases clearly with lower compressive strain rate and higher compression temperature. The result of compression test reveals that the plastic strain around 80–160 % can be obtained easily at the temperature within SCL region with strain rate around 2.5×10^{-3} to 1×10^{-2} s^{-1}. A typical deformed sample at 458 K with a strain rate of 1×10^{-2} s^{-1} is shown in Figure 5. Moreover, the results of X-ray diffraction reveal that the $Mg_{58}Cu_{31}Y_6Nd_5$ BMG rods

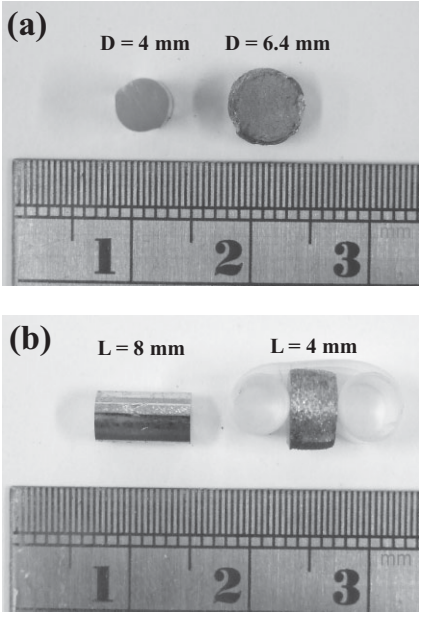

Fig. 5. The $Mg_{58}Cu_{31}Y_6$ Nd_5 rod deformed at 458 K with a strain rate 1×10^{-2} s^{-1}; a) top view, b) side view.

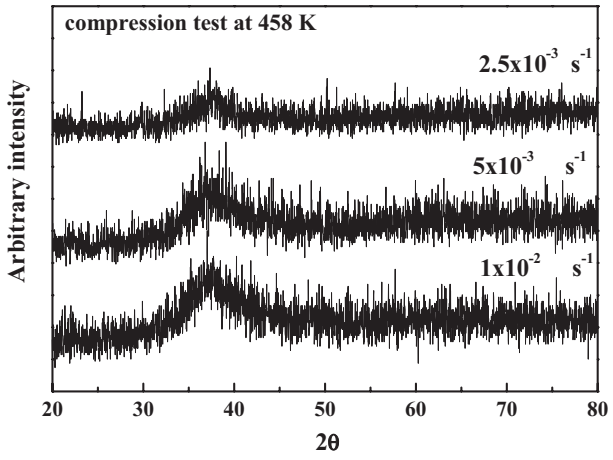

Fig. 6. X-ray diffraction patterns of $Mg_{58}Cu_{31}Y_6$ Nd_5 BMG rods after compression test at 458 K with strain rate of 2.5×10^{-3}–1×10^{-2} s^{-1}

remain in the amorphous state after compression at 458 K with different strain rates (Fig. 6).

To discuss the flow behavior of the Mg-based BMG further, the Backofen function is introduced (Eq. (1)),[26]

$$\sigma_{flow} = K\dot{\varepsilon}^{m} \tag{1}$$

where σ^{flow} is the flow stress, K is a constant, ε is strain rate and m is the strain sensitivity exponent. Plots of the flow stress ($\ln\sigma$) as a function of strain rate ($\ln\varepsilon$) at different temperatures are shown in Figure 7. The strain rate sensitivity exponent (m), which approached 1.0, can be obtained from the slope of the curve for the $Mg_{58}Cu_{31}Y_6Nd_5$ BMG deformed at 448, 453, and 458 K. Considering that the m value is usually below 0.6 for superplastic crystalline alloys,[27] the $Mg_{58}Cu_{31}Y_6Nd_5$ BMG possesses an ideal superplasticity like that of a Newtonian fluid. To prove the excellent workability in the SCL region of the $Mg_{58}Cu_{31}Y_6Nd_5$ BMG, a BMG rod with diameter of 6 mm was extruded into a long wire with diameter of 1 mm for more than 160 mm in length at 458 K. Moreover, a microscaled hologram was fabricated by hot pressing the $Mg_{58}Cu_{31}Y_6Nd_5$ BMG from a pre-engraved

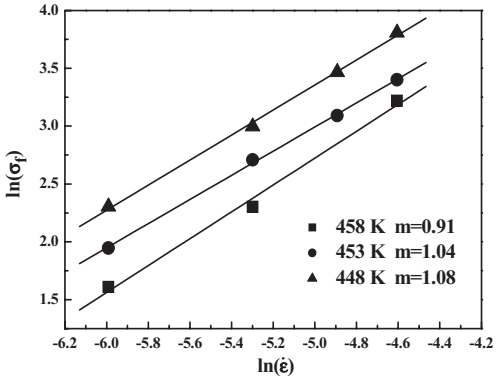

Fig. 7. Strain rate sensitivity exponents (m) for $Mg_{58}Cu_{31}Y_6$ Nd_5 BMG rods obtained at different temperatures.

© 2008 WILEY-VCH Verlag GmbH & Co. KGaA, Weinheim

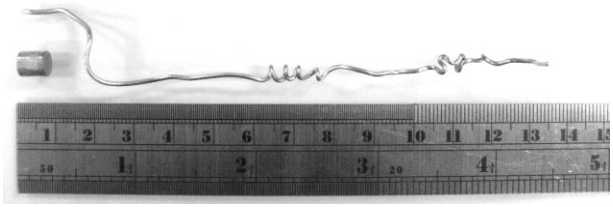

Fig. 8. A $Mg_{58}Cu_{31}Y_6$ Nd_5 metallic glass wire with diameter of 1 mm and length of more than 160 mm fabricated by extruding the 6 mm diameter BMG rod at 458 K.

die (with microscaled groove) at 458 K in the supercooled iquid region, as shown in Figure 9(a). The replication of a hologram pattern with 100 nm depth also shows extremely good microforming ability of this $Mg_{58}Cu_{31}Y_6Nd_5$ BMG in the SCL region under suitable working conditions, as shown in Figure 9(b). The easy formation of the nanometer-scale imprinted patterns of the bulk glassy alloys is important for the future application in high-density recording and storage materials.[28]

Conclusion

According to the results of DSC, TMA, and hot compression tests, the deformation behavior of the $Mg_{58}Cu_{31}Y_6Nd_5$ BMG within the SCL region reveals a relatively low viscosity between 10^6 and 10^7 Pa s within the SCL region. The plastic strain around 80–160 % can be obtained easily by a compression test within the SCL region at different strain rates. In addition, the results of X-ray diffraction show that the $Mg_{58}Cu_{31}Y_6Nd_5$ BMG sample keeps its amorphous state after compression at 458 K at different strain rates. In parallel, a strain rate sensitivity exponent (m) approaching 1.0 can be obtained for the $Mg_{58}Cu_{31}Y_6Nd_5$ BMG deformed at 448, 453, and 458 K. This result proves that this $Mg_{58}Cu_{31}Y_6Nd_5$ BMG behaves with an ideal superplasticity like that of a Newtonian fluid body. The replication of a hologram pattern with 100 nm depth also shows the extremely good microforming ability of this $Mg_{58}Cu_{31}Y_6Nd_5$ BMG in the SCL region under suitable working conditions.

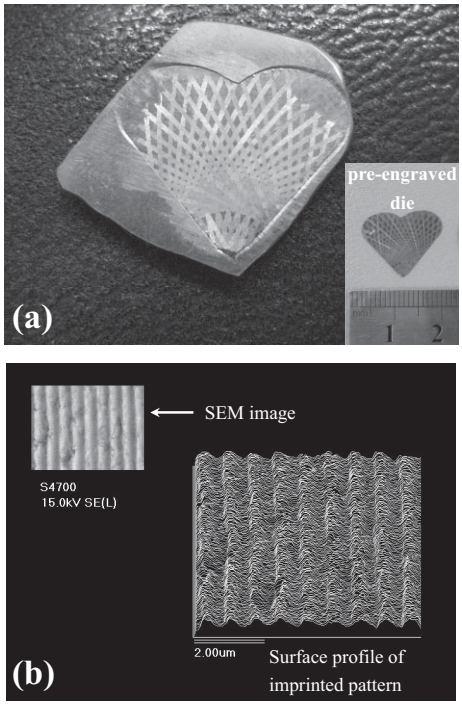

Fig. 9. The $Mg_{58}Cu_{31}Y_6Nd_5$ BMG: Photographs of a) pre-engraved die and imprinted hologram pattern at 458 K; b) SEM secondary electron image and surface profile of the imprinted hologram pattern.

Received: April 07, 2008
Final version: July 03, 2008
Published online: November 13, 2008

[1] A. A. Lou, *J. Met.* **2002**, *54*, 42.
[2] M. O. Pekguleryuz, H. Kaplan, R. Neelameggham, J. Hryn, B. Powell, G. Cole, J. F. Nie, *J. Met.* **2002**, *54*, 18.
[3] D. L. Albright, F. Bergeron, R. Neelameggham, A. A. Luo, H. Kaplan, M. O. Pekguleryuz, *J. Met.* **2002**, *5*, 22.
[4] A. Inoue, A. Kato, T. Zhang, S. G. Kim, T. Masumoto, *Mater. Trans. JIM.* **1991**, *32*, 609.
[5] A. Inoue, T. Nakamura, N. Nishiyama, T. Masumoto, *Mater. Trans. JIM.* **1992**, *33*, 937.
[6] E. S. Park, H. G. Kang, W. T. Kim, D. H. Kim, *J. Non-Cryst. Solids* **2001**, *279*, 154.
[7] L. J. Chang, J. S. C. Jang, B. C. Yang, J. C. Huang, *J. Alloy Comp.* **2007**, *434–435*, 221.
[8] H. Men, Z. Q. Hu, J. Xu, *Scr. Mater.* **2002**, *46*, 699.
[9] K. Amiya, A. Inoue, *Mater. Trans. JIM* **2000**, *41*, 1460.
[10] K. Amiya, A. Inoue, *Mater. Trans.* **2001**, *42*, 543.
[11] H. Men, W. T. Kim, D. H. Kim, *J. Non-Cryst. Solids* **2004**, *337*, 29.
[12] T. H. Hung, Y. C. Chang, H. M. Chen, Y. L. Tsai, J. C. Huang, J. S. C. Jang, T. G. Nieh, *Mater. Sci. Forum.* **2007**, *539–543*, 1926.
[13] G. Yuan, A. Inoue, *J. Alloy Comp.* **2005**, *327*, 134.
[14] X. K. Xi, R. J. Wang, D. Q. Zhao, M. X. Pan, W. H. Wang, *J. Non-Cryst. Solids* **2004**, *344*, 105.
[15] H. Ma, L. L. Shi, J. Xu, Y. Li, E. Ma, *Appl. Phys. Lett.* **2005**, *87*, 181915.
[16] L. J. Chang, B. C. Yang, P. T. Chiang, J. S. C. Jang, J. C. Huang, *Mater. Sci. Forum.* **2007**, *539–543*, 2106.
[17] T. H. Hung, Y. C. Chang, Y. N. Wang, C. W. Tang, J. N. Kuo, H. M. Chen, Y. L. Tsai, J. C. Huang, J. S. C. Jang, C. T. Liu, *Mater. Trans.* **2007**, *48*, 1621.
[18] J. S. C. Jang, C. C. Tseng, L. J. Chang, C. F. Chang, W. J. Lee, J. C. Huang, C. T. Liu, *Mater. Trans.* **2007**, *48*, 1684.
[19] G. Yuan, T. Zhang, A. Inoue, *Mater. Trans.* **2000**, *44*, 1460.
[20] Q. Zheng, H. Ma, E. Ma, J. Xu, *Scr. Mater.* **2006**, *55*, 541.
[21] H. M. Chen, Y. C. Chang, T. H. Hung, X. H. Du1, J. C. Huang, J. S. C. Jang, P. K. Liaw, *Mater. Trans.* **2007**, *48*, 1802.

 © 2008 WILEY-VCH Verlag GmbH & Co. KGaA, Weinheim

[22] T. Zumkley, S. Suzuki, M. Seidel, S. Mechler, M. P. Macht, *Mater. Sci. Forum.* **2002**, *386–388*, 541.
[23] Y. Saotome, K. Itoh, T. Zhang, A. Inoue, *Scr. Mater.* **2001**, *44*, 1541.
[24] Q. Jing, R. P. Liu, G. J. Shao, W. K. Wang, *Mater. Sci. Eng.* **2003**, *A359*, 402.
[25] J. Schroers, Q. Pham, A. Desai, *J. Microelectromech. Syst.* **2007**, *16*, 240.
[26] W. J. Kim, D. S. Ma, H. G. Jeong, *Scr. Mater.* **2003**, *49*, 1067.
[27] Y. Kawamura, T. Nakamura, H. Kato, H. Mano, A. Inoue, *Mater. Sci. Eng.* **2001**, *A304*, 674.
[28] A. Inoue, A. Takeuchi, *Mater. Sci. Eng.* **2004**, *A375–377*, 16.

 © 2008 WILEY-VCH Verlag GmbH & Co. KGaA, Weinheim